Dalton Transactions

PAPER

View Article Online
View Journal | View Issue

Cite this: *Dalton Trans.*, 2016, **45**, 18892

Structure and thermodynamic stability of UTa_3O_{10}, a U(v)-bearing compound†

Xiaofeng Guo,[a,b] Christian Lipp,[c] Eitan Tiferet,[d] Antonio Lanzirotti,[e] Matthew Newville,[e] Mark H. Engelhard,[f] Di Wu,[g] Eugene S. Ilton,[h] Stephen R. Sutton,[e,i] Hongwu Xu,[a] Peter C. Burns[c,j] and Alexandra Navrotsky*[b]

Received 18th July 2016,
Accepted 8th September 2016

DOI: 10.1039/c6dt02843h

www.rsc.org/dalton

Heating a mixture of uranyl(vi) nitrate and tantalum(v) oxide in the molar ratio of 2 : 3 to 1400 °C resulted in the formation of a new compound, UTa_3O_{10}. The honey colored to yellow brown crystals of UTa_3O_{10} crystallize in an orthorhombic structure with the space group *Fddd* (no. 70), lattice parameters a = 7.3947(1), b = 12.7599(2), c = 15.8156(2) Å, and Z = 8. Vertex sharing $[TaO_6]^{7-}$ octahedra of two crystallographically distinct Ta cations form a three dimensional tantalate framework. Within this framework, six membered rings of $[TaO_6]^{7-}$ octahedra are formed within the (001) plane. The center of these rings is occupied by the uranyl cations $[UO_2]^{+}$, with an oxidation state of +5 for uranium. The pentavalence of U and Ta was confirmed by X-ray photoelectron spectroscopy and X-ray adsorption spectroscopy. The enthalpy of formation of UTa_3O_{10} from Ta_2O_5, β-U_3O_7, and U_3O_8 has been determined to be 13.1 ± 18.1 kJ mol^{-1} using high temperature oxide melt solution calorimetry with sodium molybdate as the solvent at 700 °C. The close to zero enthalpy of formation of UTa_3O_{10} can be explained by closely balanced structural stabilizing and destabilizing factors, which may also apply to other UM_3O_{10} compounds.

Introduction

Like other metal uranate systems,[1–7] UM_3O_{10} compounds are able to incorporate uranium in different oxidation states. Compared to U(iv) or U(vi), U(v) is far less well characterized in solids,[8–10] especially in oxides,[5–7] from both structural and thermodynamic perspectives. As the intermediate valence state between the insoluble U(iv) and highly soluble U(vi), U(v) can play a transitional role kinetically and/or thermodynamically in mobilization or immobilization of U.[11] The U(v)-bearing compounds could also serve as precursors for forming many other uranium minerals.[12] Since tantalum is pentavalent, the uranium in UTa_3O_{10} has a nominal pentavalent oxidation state. Similar to $MU(v)O_4$ [5,6,13] compounds, UTa_3O_{10} is of fundamentally interest in its chemistry and structure. Actinides such as U and Th can enter tantalate structure to form UTa_2O_8-like mineral[14] and other synthetic compounds.[15–20] So in terms of uranium geochemistry or contamination remediation, study of how U(v) immobilizes in this crystalline tantalate system can be potentially useful for understanding similar phases formed in the environment.

UV_3O_{10} [21] contains shorter U–O bonds than those in $U(v)Nb_3O_{10}$, indicating it contains U(vi) and mixed oxidation states for vanadium. USb_3O_{10} has the same structure type[22] and is a catalyst for the oxidation of alkenes and aromatic hydrocarbons.[23–31] However, only a few actinide tantalate compounds have been reported. Reactions of actinide dioxides with tantalum(v) and niobium(v) oxide yielded tantalate and niobate powders.[32] The compound UTa_3O_{10} was first reported in 1965,[33] and two years later UV_3O_{10}, UNb_3O_{10} and UTa_3O_{10} were reported to be isostructural, crystallizing in orthorhombic space group *Fddd* (no. 70) with Z = 8.[34] For UNb_3O_{10}, a complete structure determination based on single crystal X-ray

[a]*Earth and Environmental Sciences Division, Los Alamos National Laboratory, Los Alamos, New Mexico 87545, USA*
[b]*Peter A. Rock Thermochemistry Laboratory and NEAT ORU, University of California, Davis, California 95616, USA. E-mail: anavrotsky@ucdavis.edu*
[c]*Department of Civil and Environmental Engineering and Earth Sciences, University of Notre Dame, 156 Fitzpatrick Hall, Notre Dame, Indiana 46556, USA*
[d]*Nuclear Research Center – Negev Be'er-Sheva 84190, Israel Institution, Israel*
[e]*Center for Advanced Radiation Sources, University of Chicago, Chicago, Illinois 60637, USA*
[f]*Environmental Molecular Sciences Laboratory, Pacific Northwest National Laboratory, Richland, Washington 99354, USA*
[g]*The Gene and Linda Voiland School of Chemical Engineering and Bioengineering, Washington State University, Pullman, Washington 99163, USA*
[h]*Pacific Northwest National Laboratory, Richland, Washington 99352, USA*
[i]*Department of Geophysical Sciences, University of Chicago, Chicago, Illinois 60637, USA*
[j]*Department of Chemistry and Biochemistry, University of Notre Dame, Notre Dame, Indiana 46556, USA*

†Electronic supplementary information (ESI) available. See DOI: 10.1039/c6dt02843h

diffraction data followed a year later,[35] with the conclusion that the uranium in this compound is in the hexavalent oxidation state and that niobium assumes tetravalent and pentavalent oxidation states, as would be required for charge balance. In contrast, a later study concluded the oxidation states in UNb_3O_{10} are U(v) and Nb(v).[36]

Here we examine the structure and thermodynamics of the uranium tantalate UTa_3O_{10}, which we have obtained as a pure phase. The local structure of U has been determined by analyzing extended X-ray adsorption fine structure (EXAFS) and is consistent with results from crystallographic data obtained in this study. The oxidation state of U has been determined by X-ray photoelectron spectroscopy (XPS) and X-ray adsorption near edge spectroscopy (XANES), and both measurements indicate the presence of pentavalent uranium in UTa_3O_{10}.

U(v) has been demonstrated to be quite stable in several solid compounds (*e.g.* MUO_4,[5] Ca–U–Zr–Fe garnets[37]), and these phases may be suitable for long term storage of uranium. Thus determining whether the thermodynamics of UTa_3O_{10} is analogously favorable is of interest. We have conducted high temperature oxide melt solution calorimetry to determine the enthalpies of formation of UTa_3O_{10} from oxides and elements. The thermodynamic behavior was compared to that of other U(v)-containing compounds and discussed from structural perspectives.

Table 1 UTa_3O_{10}: crystallographic data

Crystal system	Orthorhombic
Space group	*Fddd* (no. 70)
Lattice parameters[a] (in Å)	a = 7.3947(1) b = 12.7599(2) c = 15.8156(2)
Number of formula units	Z = 8
Calculated density[a] (D_x in g cm^{-3})	8.376
Molar volume[a] (V_m in cm^3 mol^{-1})	112.33
Diffractometer, wavelength	Bruker APEXII, Mo-Kα: λ = 0.7107 Å
Index range ($\pm h_{max}$, $\pm k_{max}$, $\pm l_{max}$)	10, 18, 22
$2\theta_{max}$ (in grd)	60.9
F(000)	3128
Absorption coefficient μ (in mm^{-1})	65.52
Data correction	Background, polarization and Lorentz factors; numerical absorption correction: program X-SHAPE[47]
Observed reflections	6414
Unique reflections	567
R_{int}/R_σ	0.042/0.017
Reflections with $\lvert F_o\rvert \geq 4\sigma(F_o)$	423
Structure determination and refinement	Program package SHELX-97[48]
Scattering factors	International Tables, vol. C[49]
R_1/R_1 with $\lvert F_o\rvert \geq 4\sigma(F_o)$	0.026/0.017
wR_2/Goodness of fit (GooF)	0.047/1.065
Extinction (g)	0.00011(1)
Residual electron density max./min. (ρ in e$^-$ 10^{-6} pm^{-3})	2.36/−1.42

[a] Further details of the crystal structure investigation can be obtained from the Fachinformationszentrum (FIZ) Karlsruhe, D-76344 Eggenstein-Leopoldshafen, Germany (Fax: +49(0)7247/808-666; E-mail: crysdata@fiz-karlsruhe.de), on quoting the depository number CSD 422449 for UTa_3O_{10}.

Experimental methods

Synthesis and structural analysis

Crystals of UTa_3O_{10} were obtained when uranyl(VI) nitrate hexahydrate $[UO_2][NO_3]_2{\cdot}6H_2O$ (International Bio-Analytical Industries Inc.; 99.9%) and tantalum(v) oxide (Ta_2O_5: Sigma-Aldrich; 99.99%) in a molar ratio of 2 : 3 were heated in a tube furnace at 1400 °C for 2 h. The temperature was then lowered to 900 °C at 3 °C h^{-1}, and then reduced to room temperature at a rate of 100 °C h^{-1}. The reactants were contained in a high-alumina crucible and lid. A honey colored crystal with a platy habit was selected for single crystal X-ray diffraction data collection using an APEXII diffractometer (Bruker). Details and results of the structural analysis are presented in Tables 1–3. Chemical composition and sample homogeneity were checked with electron probe microanalysis (EPMA) using a Cameca SX50 coupled with wavelength dispersive spectrometry (WDS), at an accelerating voltage of 20 keV, a probe current of 10 nA and a spot size of 1 μm. Quantitative WDS was conducted using a lower accelerating voltage of 15 keV. UO_2, and Ta_2O_5 were used as analytical standards for U and Ta, respectively. For the spectroscopy and calorimetry described below, powdered samples were used. To confirm the sample purity, powder X-ray diffraction was carried out by grinding 5 mg of UTa_3O_{10} crystals into a fine powder with ethanol and depositing the paste onto a zero-background quartz slide. The diffraction pattern was collected from 16 to 83° in 2θ with a step size of 0.011° and a collection time of 2 s per step using a Bruker D8 Advance diffractometer equipped with Cu $K_{\alpha1}$ radiation and a solid state detector.

X-ray photoelectron spectroscopy (XPS)

XPS was performed using a Kratos Axis DLD spectrometer equipped with a monochromatic X-ray source of Al K_α source (15 mA, 14 keV). The instrument work function was calibrated to give a binding energy (BE) of 83.96 ± 0.05 eV for the Au $4f_{7/2}$ line for metallic gold and the spectrometer dispersion was adjusted to give a BE of 932.62 ± 0.05 eV for the Cu $2p_{3/2}$ line of metallic copper. High resolution analyses were carried out with an analysis area of 300 × 700 microns and a pass energy of 80 eV. The Kratos charge neutralizer system was used on all specimens. Spectra have been charge corrected to the main line of the carbon 1s spectrum (adventitious carbon) which was set to 285.0 eV. Spectra were analyzed using CasaXPS software (version 2.3.16 PR 1.6).

X-ray absorption spectroscopy

The oxidation state of uranium was determined by XANES spectroscopy at the GSECARS X-ray microprobe beamline (13-ID-E) at the Advanced Photon Source (APS), Argonne National Laboratory (Argonne, IL USA). XANES spectra were collected in transmission mode using a 200 mm long, helium filled ion chamber to monitor incident flux,

Table 2 Atomic coordinates and coefficients of the anisotropic thermal displacement parameters[a] (U_{ij}/Å^2) for UTa_3O_{10}

Atom	Wyckoff-Lage	x/a	y/b	z/c
U	8a	0	0	0
Ta1	8b	0	0	1/2
Ta2	16g	0	0	0.26044(2)
O1	32h	0.2979(7)	0.1004(4)	0.0025(3)
O2	16g	0	0	0.3759(3)
O3	16g	0	0	0.1167(3)
O4	16f	0	0.2028(5)	0

Atom	U_{11}	U_{22}	U_{33}	U_{23}	U_{13}	U_{12}
U	0.0140(3)	0.0171(2)	0.0034(2)	0	0	0
Ta1	0.0057(3)	0.0176(2)	0.0134(2)	0	0	0
Ta2	0.0104(2)	0.0094(2)	0.0105(2)	0	0	−0.0040(1)
O1	0.0429(27)	0.0264(23)	0.0203(19)	0.0027(16)	0.0003(19)	0.0208(23)
O2	0.0204(42)	0.0241(39)	0.0127(28)	0	0	−0.0066(53)
O3	0.0268(44)	0.0294(41)	0.0098(23)	0	0	−0.0015(58)
O4	0.0192(35)	0.0513(40)	0.0183(26)	0	0.0040(26)	0

[a] U_{ij}, defined as coefficients in the expression: $\exp[-2\pi^2(a^{*2}h^2U_{11} + b^{*2}k^2U_{22} + c^{*2}l^2U_{33} + 2b^*c^*klU_{23} + 2a^*c^*hlU_{13} + 2a^*b^*hkU_{12})$.

Table 3 Selected interatomic distances (d/Å) angles (∢/°) in UTa_3O_{10}

U–O3	1.846(5) 2×	Ta1–O2	1.963(4) 2×
U–O1	2.549(6) 4×	Ta1–O1	1.969(4) 4×
U–O4	2.588(7) 2×		
		Ta2–O2	1.826(4)
		Ta2–O4	1.951(2) 2×
		Ta2–O1	1.952(4) 2×
		Ta2–O3	2.273(5)
O3–U–O3	180	O2–Ta1–O2	180
O3–U–O1	89.1(1) 4×	O2–Ta1–O1	88.9(1) 4×
O3–U–O4	90 4×	O2–Ta1–O1	91.1(1) 4×
O3–U–O1	90.9(1) 4×	O1–Ta1–O1	81.2(3) 2×
O1–U–O4	59.8(1) 4×	O1–Ta1–O1	98.8(3) 2×
O1–U–O1	60.4(2) 2×	O1–Ta1–O1	177.7(3) 2×
O1–U–O1	119.6(2) 2×		
O1–U–O4	120.2(1) 4×	O2–Ta2–O3	180
O1–U–O1	178.2(2) 2×	O2–Ta2–O4	94.85(1) 4×
O4–U–O4	180	O2–Ta2–O1	96.0(1) 4×
		O3–Ta2–O1	84.0(1) 2×
		O3–Ta2–O4	85.15(1) 2×
		O1–Ta2–O4	82.0(3)2×
		O1–Ta2–O4	96.9(3) 2×
		O1–Ta2–O1	168.0(3)
		O4–Ta2–O4	170.29(2)

I_0 (ADC IC-400-200) and a 50 mm long nitrogen filled ion chamber downstream of the sample to monitor transmitted flux, I_1 (ADC 500-50). XANES spectra were obtained by scanning a Si(111) monochromator through the U L_{III} absorption edge (~17 166 eV) and recording the total absorption. In the XANES region the energy step sizes were 2.5 eV from 17 066 to 17 146 eV and 0.25 eV from 17 146 to 17 191 eV. The EXAFS portion of the spectra was then collected to a distance of 15 Å^{-1}. Dwell time at each energy step was 1 s, and up to eight spectra were collected and summed to improve signal-to-noise ratios. Energy calibration was obtained using a Y metal foil (first derivative peak defined to be 17 037 eV). The samples were prepared as thin powder layers mounted between Scotch tape. The X-ray absorption spectroscopy data processing software Athena[38] was used for analysis, and software Artemis[38] was used for EXAFS fitting.

Calorimetry

A ~5 mg pellet of UTa_3O_{10} was dropped from room temperature into molten sodium molybdate ($3NaO{\cdot}4MoO_3$) solvent at 702 °C in a custom built Tian-Calvet twin microcalorimeter.[39,40] Oxygen gas was continuously bubbled through the melt at 5 ml min^{-1} to ensure an oxidizing environment and facilitate dissolution, and to stir the melt and prevent local saturation.[41] In addition, flowing oxygen gas at ~50 ml min^{-1} was continuously flushed through the calorimeter glassware assembly to maintain a constant gas environment above the solvent and remove any evolved gases.[41] Upon rapid and complete dissolution of the sample, the enthalpy of drop solution, ΔH_{ds}, was obtained. Dissolution of uranium oxides and some other uranium containing compounds have been demonstrated in this solvent, and their drop solution enthalpy data were obtained previously.[4,5,37,42–45] Because Ta_2O_5 is very refractory and slow to dissolve in molten salt solvents, McHale and Navrotsky[46] used a thermochemical cycle involving oxidation of Ta metal to derive ΔH_{ds} of Ta_2O_5 in $3NaO{\cdot}4MoO_3$ solvent at 702 °C. Finally, using appropriate thermochemical cycles (Table 5), the enthalpies of formation of UTa_3O_{10} from its constituent oxides ($\Delta H_{f,ox}$ and $\Delta H'_{f,ox}$) and standard enthalpy $\left(\Delta H_f^\circ\right)$ were calculated. The equipment, calibration and experimental method have been described in detail elsewhere.[39,40]

Results and discussion

Crystal structure

UTa_3O_{10} crystallizes in space group *Fddd* (no. 70) with a = 7.3947(1), b = 12.7599(2), c = 15.8156(2) Å and Z = 8 (Tables 1–3, Fig. 1). For better comparison with related structures the non-centrosymmetric setting of space group

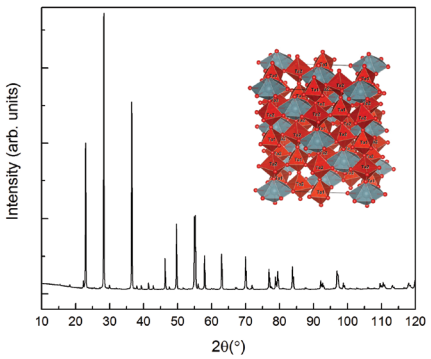

Fig. 1 Powder XRD patterns of UTa_3O_{10}.

Fddd was chosen, as for UNb_3O_{10} and UV_3O_{10} previously.[21,35,36] Whereas uranium occupies special site 8a, there are two crystallographically distinct Ta^{5+} cations. These are on sites 8b and 16g, and both are surrounded by six O^{2-} anions in the shape of $[TaO_6]^{7-}$ octahedra. Designations of the O atoms are as used earlier for UNb_3O_{10} (and UV_3O_{10} [21] and USb_3O_{10} [22]).

The $[(Ta1)O_6]^{7-}$ octahedron is almost regular, with apical Ta1–O2 bond lengths of 1.96 Å and equatorial Ta1–O1 bond lengths of 1.97 Å. The equatorial $(O1)^{2-}$ anions are not arranged in a square, as evident in the (O1–Ta1–O1) angles that are 81 and 99°. The octahedron about Ta2 is more distorted, most notably by displacement of tantalum out of the equatorial (O1,O1,O4,O4) plane, which results in a short Ta2–O2 distance of 1.83 Å and a relatively long 2.27 Å for Ta2–O3. The bond lengths of the equatorial oxygen atoms O1 and O2 are similar to those of the $[(Ta1)O_6]^{7-}$ octahedron, at 1.95 Å. This type of octahedral distortion also occurs in the isostructural vanadium,[21] niobium[35,36] and antimony[22] compounds. Compared to the apical V1–O2 distances of 2.01 Å, considerable distortion occurs as the V2–O2 and V2–O3 distances are 1.70 Å and 2.62 Å. The more recently determined structure of UNb_3O_{10} [36] indicates values that are closer to the tantalum compound. In this case, the Nb1–O2 distances are 1.97 Å, and Nb2–O2 and Nb2–O3 are 1.85 and 2.21 Å. In USb_3O_{10} [22] the apical bond lengths are 1.85 Å (Sb1–O2) and the others are 1.88 Å (Sb2–O2) as well as 2.17 Å (Sb2–O3).

As in UNb_3O_{10}, the octahedra are linked into a framework, and uranium cations reside within voids. Corner-sharing $[(Ta2)O_6]^{7-}$ octahedra form zigzag chains that extend along [100] that are connected by $[(Ta1)O_6]^{7-}$ octahedra in the (001) plane, giving $^{2}_{\infty}\{[(Ta1)(Ta2)_2O_{12}]^{9-}\}$ sheets. Triangular and hexagonal voids occur within these sheets. Attachment of these sheets in the [001] direction is through common oxygen corners, giving the $^{3}_{\infty}\{[(Ta1)(Ta2)_2O_{10}]^{5-}\}$ framework that requires U^{5+} to achieve charge balance.

Uranium occupies hexagonal voids in the $^{3}_{\infty}\{[(Ta1)(Ta2)_2O_{10}]^{5-}\}$ framework, surrounded by eight oxygen atoms arranged in a hexagonal bipyramid. The U–O distances in the equatorial plane are 2.55 and 2.59 Å for U–O1 and U–O4, respectively. The apical U–O bond lengths are much shorter at 1.85 Å, consistent with the presence of a uranyl cation. The bond lengths about the uranium cations are longer than those expected for U(VI), and the bond valence sum calculated using R_{ij} = 2.042 and b = 0.506 Å (ref. 4 and 50) yields 5.10 valence units, consistent with occupancy of the site by U(V).

In UV_3O_{10} [21] apical bond lengths of 1.78 Å, and equatorial bond lengths of 2.46 Å and 2.48 Å give a bond valence sum at the uranium position of 5.94 valence units, indicating the site is occupied by U(VI). The corresponding value in USb_3O_{10} [22] is 5.80 valence units, which is unexpected in the event that all of the Sb present is pentavalent. For UNb_3O_{10}, Gasperin *et al.*[35] report U–O bond lengths of 1.95 Å for the uranyl cation. The bond valence sum at the uranium site is 5.00 valence units, although the article concluded that all of the uranium is hexavalent. In another study, Dickens *et al.*[36] reported slightly shorter uranyl U–O bonds of 1.88 Å, but the bond valence sum at the uranium site was 4.7 valence units. Their magnetic measurements for UNb_3O_{10} were consistent with a pentavalent oxidation state for uranium.

Determination of U and Ta oxidation states

The oxidation state assignment of U(V) in UTa_3O_{10} from crystal structure analysis was confirmed by spectroscopic studies. The

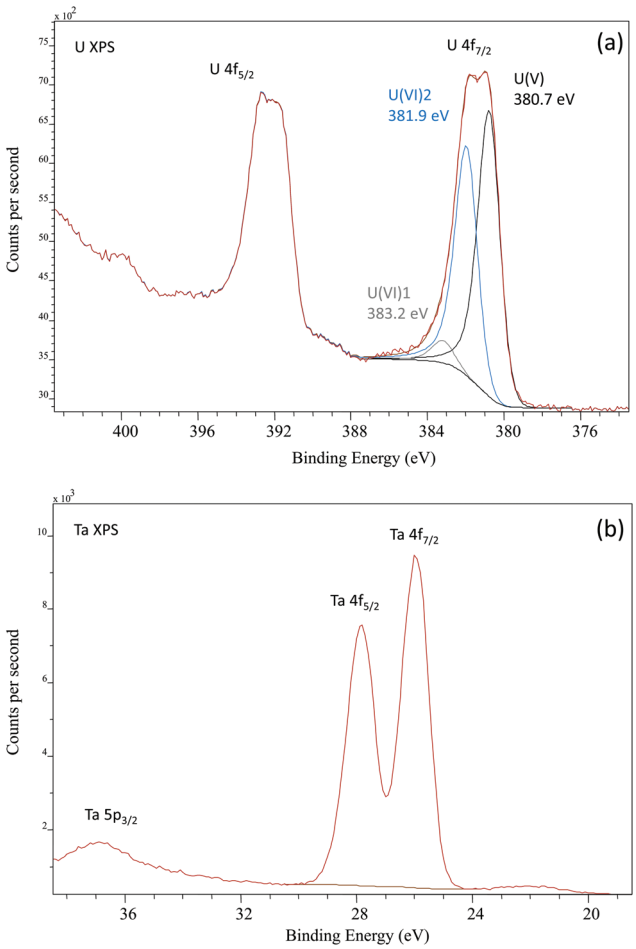

Fig. 2 4f region XPS spectra of U (above) and Ta (bottom) of UTa_3O_{10}.

Table 4 U oxidation state obtained from fitting XPS spectrum of UTa_3O_{10}

Sample	U(VI)1		U(VI)2		U(VI) Total	U(V)		U (apfu)
	mol%	BE(eV)	mol%	BE(eV)		mol%	BE(eV)	
UTa_3O_{10}	4.2	383.3	42.7	381.9	46.9	53.1	380.7	0.8

oxidation states of U and Ta in UTa_3O_{10} were first determined by XPS. The obtained spectra are shown in Fig. 2. CasaXPS software V2.3.16 was used to fit the U $4f_{7/2}$ line after Shirley background subtraction. In the spectrum of U, the U $4f_{7/2}$ line has one BE peak for U(V) at 380.7 eV, and two BE peaks for U(VI) at 381.9 and 383.2 eV. This is consistent with U spectrum in other U(V)-containing compounds. The quantitative analysis shows that the U(V)/U ratio of UTa_3O_{10} is 53.1% (Table 4). However, because XPS is sensitive to the near surface (top ~10 nm of a solid), this result may be due to surface oxidation and may not represent the bulk. The Ta spectrum provides additional support for this argument. In Fig. 2-b, Ta $4f_{7/2}$ has a BE peak located at 26.0 eV, consistent with a high oxidation state of Ta(V). Thus, the combined XPS results suggest the existence of pentavalent U in the sample.

U L_{III} XANES characterizes bulk oxidation state. However, the difference between absorption edge energy (E_0) of U(V) and that of U(VI) is subtle in XANES, on the order of 0.8–2.0 eV.[3,5,51–53] In this study, we compare the XANES spectrum of U in UTa_3O_{10} with those in MUO_4 (M = Mg, Cr, Fe)[5] for a qualitative characterization of bulk U. The U L_{III} XANES spectrum were collected on UTa_3O_{10} (Fig. 3), with E_0 = 17 169.5 eV. Because U(V) has a lower core electron binding energy, this edge energy is lower than that of U(VI) in Mg**U(VI)**O_4, E_0 = 17 170.4 eV.[5] The measured edge energy is also consistent with that of U(V) in Cr**U(V)**O_4 or Fe**U(V)**O_4,[5] which may reflect that the edge energies of U in these systems are similar despite of the different chemical environments or binding characteristics. Combined with results from XPS, we concluded the dominant existence of U(V) in UTa_3O_{10}. In addition, the fitting of U EXAFS gives bond distances between uranium and its first coordinated oxygen: 1.883 Å for U–O3, 2.521 Å for U–O1, and 2.555 Å for U–O4. The fitted U–O bond lengths in the first shell are in agreement with those obtained from single crystal structural analysis (Table 3).

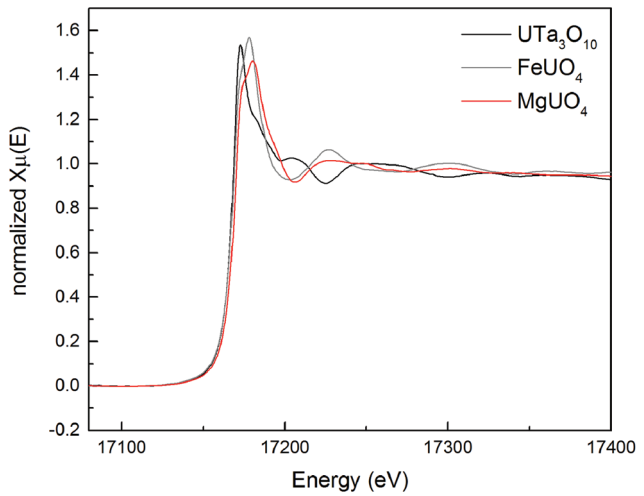

Fig. 3 U L_{III} XANES spectra of UTa_3O_{10} (black), Fe**U(V)**O_4[5] (gray), and Mg**U(VI)**O_4[5] (red).

Thermodynamic analysis

The measured enthalpies of drop solution, ΔH_{ds}, are listed in Table 5. For a direct comparison of U(V) energetics to phases containing only U(IV) and U(VI), the enthalpy of formation, $\Delta H_{f,ox}$, of UTa_3O_{10} from its constituent binary oxides (γ-UO_3, UO_2, Ta_2O_5) is 1.2 ± 18.1 kJ mol^{-1}, which was derived by combining the measured ΔH_{ds} of UTa_3O_{10} with other known ΔH_{ds} for the auxiliary oxides based on the thermochemical cycles in Table 5. The derived standard enthalpy of formation of UTa_3O_{10} from the elements is −4285.4 ± 20.4 kJ mol^{-1}.

One can also calculate the enthalpy of formation of UTa_3O_{10} with respect to another U oxides assemblage (U_3O_8, β-U_3O_7) which represents the equilibrium phases closed to O/U = 2.5,

$$1/6\ U_3O_8 + 1/6\ \beta\text{-}U_3O_7 + 3/2\ Ta_2O_5 \rightarrow UTa_3O_{10} \quad (1)$$

The enthalpy of this reaction, 13.1 ± 18.1 kJ mol^{-1}, suggests the metastability of the uranium tantalate phase.

U_3O_8 is the thermodynamically stable uranium oxide phase under many natural conditions and the geological end product for many U minerals.[12] Thus long term stability of UTa_3O_{10} might be controlled by the reaction,

$$1/3\ U_3O_8 + 3/2\ Ta_2O_5 \rightarrow UTa_3O_{10} + 1/12\ O_2 \quad (2)$$

for which ΔH is calculated to be 38.5 ± 18.1 kJ mol^{-1}. Although this reaction has a positive entropy change due to the release of oxygen gas, the large positive ΔH is unlikely to be compensated by the $T\Delta S$ term, especially near ambient temperature. This result implies the likely instability of UTa_3O_{10} in nature and that it tends to decompose to its binary oxides.

Like UNb_3O_{10}, UV_3O_{10}, and USb_3O_{10}, the structure of UTa_3O_{10} has U in a hexagonal bipyramid coordinated environment, featuring two U(V)–O bonds that are shorter than the remaining equatorial U–O bonds. As a result, compared to the Ta2–O3 bond, these short apical U–O3 bonds have more electron charges distributed on the "yl" oxygen ion and are expected to display more covalent character. This feature has also been found in other MUO_4 with M as the metal with weak Lewis acidity that further increases the basicity of this "yl"

Table 5 Thermochemical cycles for determination of the enthalpies of formation of the UTa_3O_{10} from binary oxides at 25 °C

Reaction	ΔH (kJ mol^{-1})
(1) $UTa_3O_{10\,(s,\ 25\ °C)} + 1/4\ O_{2(g,702\ °C)} \rightarrow UO_{3(sln,702\ °C)} + 3/2\ Ta_2O_{5(sln,702\ °C)}$	$\Delta H_1 = \Delta H_{ds} = 103.19^a \pm 2.63^b(7)^c$
(2) γ-$UO_{3(s,\ 25\ °C)} \rightarrow UO_{3(sln,\ 702\ °C)}$	$\Delta H_2 = 9.49 \pm 1.53(2)$[42,44]
(3) $UO_{2(s,\ 25\ °C)} + 1/2\ O_{2(g,\ 702\ °C)} \rightarrow UO_{3(sln,\ 702\ °C)}$	$\Delta H_3 = -140.40 \pm 2.67(4)$[44]
(4) $U_{(s,\ 25\ °C)} + 3/2\ O_{2(g,\ 25\ °C)} \rightarrow \gamma$-$UO_{3(s,\ 25\ °C)}$	$\Delta H_4 = -1223.8 \pm 0.8$[55]
(5) $2Ta_{(s,\ 25\ °C)} + 5/2\ O_{2(g,\ 25\ °C)} \rightarrow Ta_2O_{5(s,\ 25\ °C)}$	$\Delta H_5 = -2041.9 \pm 6.3$[56]
(6) $2Ta_{(s,\ 25\ °C)} + 5/2\ O_{2(g,\ 702\ °C)} \rightarrow Ta_2O_{5(sln,\ 702\ °C)}$	$\Delta H_6 = -1983.2 \pm 10.1$[46]
(7) $Ta_2O_{5(s,\ 25\ °C)} \rightarrow Ta_2O_{5(sln,\ 702\ °C)}$	$\Delta H_7 = 113.3 \pm 11.9^d$
(8) $1/3\ U_3O_{8(s,\ 25\ °C)} + 1/6\ O_{2(g,\ 25\ °C)} \rightarrow \gamma$-$UO_{3(s,\ 25\ °C)}$	$\Delta H_8 = -32.3 \pm 1.1$[55]
(9) $1/3\ \beta$-$U_3O_{7(s,\ 25\ °C)} \rightarrow UO_{2(s,\ 25\ °C)} + 1/6\ O_{2(g,\ 25\ °C)}$	$\Delta H_9 = 56.0 \pm 2.2$[57]
(10) $O_{2(g,\ 25\ °C)} \rightarrow O_{2(g,\ 702\ °C)}$	$\Delta H_{10} = 21.83$[58]
Thermochemical cycles	
$1/2\ \gamma$-$UO_{3(s,\ 25\ °C)} + 1/2\ UO_{2(s,\ 25\ °C)} + 3/2\ Ta_2O_{5(s,\ 25\ °C)} \rightarrow UTa_3O_{10(s,\ 25\ °C)}$	
$\Delta H_{f,ox} = -\Delta H_1 + 1/2\ \Delta H_2 + 1/2\ \Delta H_3 + 3/2\ \Delta H_7$	1.2 ± 18.1
$1/6\ U_3O_{8(s,\ 25\ °C)} + 1/6\ \beta$-$U_3O_{7(s,\ 25\ °C)} + 3/2\ Ta_2O_{5(s,\ 25\ °C)} \rightarrow UTa_3O_{10(s,\ 25\ °C)}$	
$\Delta H'_{f,ox} = \Delta H_{f,ox} + 1/2\ \Delta H_8 + 1/2\ \Delta H_9$	13.1 ± 18.1
$1/3\ U_3O_{8(s,\ 25\ °C)} + 3/2\ Ta_2O_{5(s,\ 25\ °C)} \rightarrow UTa_3O_{10(s,\ 25\ °C)} + 1/12\ O_{2(g,\ 25\ °C)}$	
$\Delta H''_{f,ox} = \Delta H_{f,ox} + 1/2\ \Delta H_8$	38.5 ± 18.1
$U_{(s,\ 25\ °C)} + 3Ta_{(s,\ 25\ °C)} + 5O_{2(g,\ 25\ °C)} \rightarrow UTa_3O_{10(s,\ 25\ °C)}$	
$\Delta H_f^\circ = \Delta H_{f,ox} + \Delta H_4 + 3/2\ \Delta H_5$	-4285.4 ± 20.4

[a] Average. [b] Two standard deviations of the average value. [c] Number of measurements. [d] Obtained from (5) and (6).

oxygen-neighboring metal cation.[5] That study also reported a positive correlation between the covalency and the energetic stability which suggests the covalency of the "uranyl" U–O bond can be a stabilizing factor for the structure.[5] Therefore, U(v), though less stable than U(vi), may be stabilized in the UM_3O_{10} structure by the presence of covalent U(v)–O bonds. This may also explain why U in UV_3O_{10} is in mixed valence states because V^{5+} is more acidic than Ta^{5+}, and also is a relatively stronger Lewis acid that competes with U(v) for electron density and decreases its basicity. Thus, its acid–base chemistry may not yield a stable phase for U(v); while in fact a mixed states of U was found as a stable form in UV_3O_{10}.

On the other hand, the covalent U–O bond extends the Ta2–O3 bond to 2.27 Å and distorts the Ta2 octahedra with displacement of Ta out of the equatorial plane. Strain energy is likely to be stored in these Ta–O bonds that are not at the strain-free distances. This is plausible; for instance, a similar phenomenon was confirmed in Fe–O bond lengths in another system (*e.g.* Ce^{4+}:YIG[54]) by DFT. In other words, the relaxation of these much shorter and longer Ta–O bonds to their strain-free status would release energy.

Another destabilizing factor may come from the edge sharing of the U hexagonal bipyramid with Ta2 octahedra. The six edges formed by equatorial oxygens are all shared by Ta2 octahedra that, according to Pauling's rule, decreases the stability of the structure. Therefore, the competition between the stabilizing and destabilizing factors may explain why UTa_3O_{10} is essentially equal in enthalpy (13.1 ± 18.1 kJ mol^{-1}) to a mixture of its binary oxides (Ta_2O_5, U_3O_8, β-U_3O_7) providing the same average uranium oxidation state. Based on the (UO_2, γ-UO_3) assemblage, the formation enthalpy of UTa_3O_{10} (1.2 ± 18.1 kJ mol^{-1}) can be compared to other reported U(v) compounds and is much less exothermic (−33.4 kJ mol^{-1} for $CrUO_4$, or −32.2 kJ mol^{-1} for $FeUO_4$).[5] Further investigation of the electronic structure of UTa_3O_{10} by density functional theory calculations may provide additional insight into this proposed mechanism for its weak energetic stability.

A review of the thermodynamics of uranium compounds[4] suggests that the energetics of different groups of metal uranium oxide systems follow similar trends against acidity of oxides or ionic radius, in which, however, each trend has a different slope. Thus, we postulate that UV_3O_{10}, UNb_3O_{10}, and UTa_3O_{10} may follow a trend of increasing stability as a function of the ionic radius of their metal cation, similar to that seen in MUO_4 systems. Fig. 4 shows the comparison of enthalpy of formation of UTa_3O_{10} and MUO_4. Further calorimetric

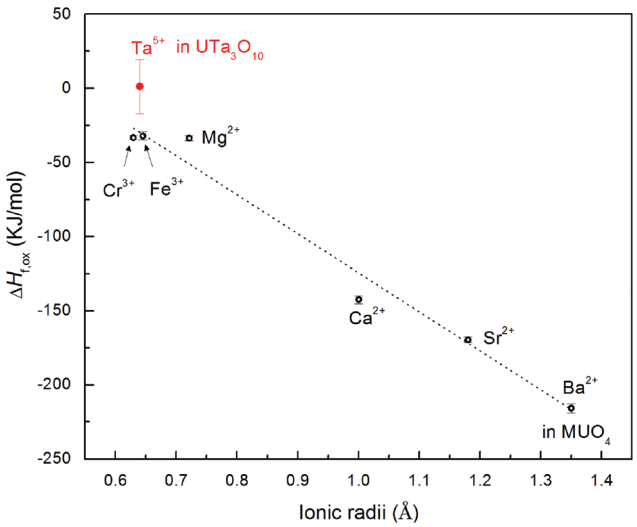

Fig. 4 The enthalpy of formation of UTa_3O_{10} compared to those of other MUO_4.[5]

measurements on other UM_3O_{10} compounds are needed to explore this possible relation.

Acknowledgements

This paper is based on work supported as part of the Materials Science of Actinides, an Energy Frontier Research Center funded by the U.S. Department of Energy, Office of Science, Office of Basic Energy Sciences under Award Number DESC0001089. X. G was also supported by a Seaborg post-doctoral fellowship from the Laboratory Directed Research and Development (LDRD) program, through the G. T. Seaborg Institute, of Los Alamos National Laboratory (LANL), which is operated by Los Alamos National Security LLC, under DOE Contract DE-AC52-06NA25396. The XAS work was performed at GeoSoilEnviroCARS (The University of Chicago, Sector 13), Advanced Photon Source (APS), Argonne National Laboratory. GeoSoilEnviroCARS is supported by the National Science Foundation – Earth Sciences (EAR-1128799) and Department of Energy – GeoSciences (DE-FG02-94ER14466). This research used resources of the Advanced Photon Source, a U.S. Department of Energy (DOE) Office of Science User Facility operated for the DOE Office of Science by Argonne National Laboratory under Contract no. DE-AC02-06CH11357. The XPS analyses were performed using EMSL, a DOE Office of Science User Facility sponsored by the Office of Biological and Environmental Research and located at Pacific Northwest National Laboratory. PNNL is operated by Battelle for the U.S. DOE under contract DE-AC06-76RLO1930. We thank Qi Liang and Mark Asta for their preliminary computational work, discussion.

Notes and references

1 K. M. Efremova, E. A. Ippolitova, I. P. Simanov and V. I. Spitsyn, *Dokl. Akad. Nauk SSSR*, 1959, **124**, 1057–1060.
2 H. R. Hoekstra and R. H. Marshall, *Adv. Chem. Ser.*, 1967, 211–227.
3 A. V. Soldatov, D. Lamoen, M. J. Konstantinovic, d. B. S. Van, A. C. Scheinost and M. Verwerft, *J. Solid State Chem.*, 2007, **180**, 54–61.
4 A. Navrotsky, T. Shvareva and X. Guo, in *Uranium – Cradle to Grave*, eds. P. C. Burns and G. E. Sigmon, Mineralogical Association of Canada, Winnipeg, MB, Cananda, 2013, vol. Short Course, ch. 5, pp. 147–164.
5 X. Guo, E. Tiferet, L. Qi, J. M. Solomon, A. Lanzirotti, M. Newville, M. H. Engelhard, R. K. Kukkadapu, D. Wu, E. S. Ilton, M. Asta, S. Sutton, H. Xu and A. Navrotsky, *Dalton Trans.*, 2016, **45**, 4622–4632.
6 K. Popa, D. Prieur, D. Manara, M. Naji, J. F. Vigier, P. M. Martin, O. D. Blanco, A. C. Scheinost, T. Prussmann, T. Vitova, P. E. Raison, J. Somers and R. J. M. Konings, *Dalton Trans.*, 2016, **45**, 7847–7855.
7 S. M. Butorin, K. O. Kvashnina, A. L. Smith, K. Popa and P. M. Martin, *Chem. – Eur. J.*, 2016, **22**, 9693–9698.
8 J. Selbin and J. D. Ortego, *Chem. Rev.*, 1969, **69**, 657–671.
9 I. Grenthe, J. Drożdżyński, T. Fujino, E. C. Buck, T. E. Albrecht-Schmitt and S. F. Wolf, in *The chemistry of the actinide and transactinide elements*, ed. L. R. Morss, N. M. Edelstein and J. Fuger, Springer, Netherlands, 2008, pp. 253–698.
10 E. S. Ilton and P. S. Bagus, *SIA Surf. Interface Anal.*, 2011, **43**, 1549–1560.
11 M. Schindler, F. C. Hawthorne, M. S. Freund and P. C. Burns, *Geochim. Cosmochim. Acta*, 2009, **73**, 2471–2487.
12 R. M. Hazen, R. C. Ewing and D. A. Sverjensky, *Am. Mineral.*, 2009, **94**, 1293–1311.
13 C. M. Read, M. D. Smith and H. C. zur Loye, *Solid State Sci.*, 2014, **37**, 136–143.
14 M. Gasperin, *Bull. Soc. Fr. Mineral. Cristallogr.*, 1960, **83**, 1–21.
15 M. Gasperin, *C. R. Hebd. Seances Acad. Sci.*, 1956, **243**, 1534–1536.
16 G. Schmidt and R. Gruehn, *J. Less-Common Met.*, 1989, **156**, 75–86.
17 G. Schmidt and R. Gruehn, *J. Less-Common Met.*, 1990, **158**, 275–285.
18 J. Busch and R. Gruehn, *Z. Anorg. Allg. Chem.*, 1996, **622**, 640–648.
19 J. Busch, R. Hofmann and R. Gruehn, *Z. Anorg. Allg. Chem.*, 1996, **622**, 67–75.
20 M. Schleifer, J. Busch, B. Albert and R. Gruehn, *Z. Anorg. Allg. Chem.*, 2000, **626**, 2299–2306.
21 A. M. Chippindale, S. J. Crennell and P. G. Dickens, *J. Mater. Chem.*, 1993, **3**, 33–37.
22 R. k. Grassell, D. D. Suresh and K. Knox, *J. Catal.*, 1970, **18**, 356–358.
23 R. k. Grassell and J. L. Callahan, *J. Catal.*, 1969, **14**, 93–103.
24 R. k. Grassell and D. D. Suresh, *J. Catal.*, 1972, **25**, 273–291.
25 T. Birchall and A. Sleight, *J. Catal.*, 1978, **53**, 280–283.
26 G. W. Keulks, Z. Yu and L. D. Krenzke, *J. Catal.*, 1983, **84**, 38–44.
27 R. Delobel, H. Baussart, M. Lebras and J. M. Leroy, *J. Chem. Soc., Faraday Trans. 1*, 1984, **80**, 3331–3337.
28 J. B. Nagy, S. Maroie, H. Collette and A. Michel, *Surf. Sci.*, 1985, **163**, L693–L701.
29 J. M. Herrmann, J. Disdier, F. G. Freire and M. F. Portela, *J. Chem. Soc., Faraday Trans.*, 1995, **91**, 2343–2348.
30 S. Poulston, N. J. Price, C. Weeks, M. D. Allen, P. Parlett, M. Steinberg and M. Bowker, *J. Catal.*, 1998, **178**, 658–667.
31 S. H. Taylor, G. J. Hutchings, M. L. Palacios and D. F. Lee, *Catal. Today*, 2003, **81**, 171–178.
32 C. Keller, *J. Inorg. Nucl. Chem.*, 1965, **27**, 1233–1246.
33 M. Gasperin, *C. R. Hebd. Seances Acad. Sci.*, 1965, **261**, 3417.
34 R. Chevalie and M. Gasperin, *C. R. Acad. Sci. C. Chim.*, 1967, **265**, 1101–1103.

35 R. Chevalie and M. Gasperin, *C. R. Acad. Sci. C. Chim.*, 1968, **267**, 481–483.
36 P. G. Dickens, G. J. Flynn, S. Patat and G. P. Stuttart, *J. Mater. Chem.*, 1997, **7**, 537–543.
37 X. Guo, A. Navrotsky, R. K. Kukkadapu, M. H. Engelhard, A. Lanzirotti, M. Newville, E. S. Ilton, S. R. Sutton and H. Xu, *Geochim. Cosmochim. Acta*, 2015, **189**, 269–281.
38 B. Ravel and M. Newville, *J. Synchrotron Radiat.*, 2005, **12**, 537–541.
39 A. Navrotsky, *Phys. Chem. Miner.*, 1977, **2**, 89–104.
40 A. Navrotsky, *Phys. Chem. Miner.*, 1997, **24**, 222–241.
41 A. Navrotsky, R. P. Rapp, E. Smelik, P. Burnley, S. Circone, L. Chai and K. Bose, *Am. Mineral.*, 1994, **79**, 1099–1109.
42 K. B. Helean, A. Navrotsky, E. R. Vance, M. L. Carter, B. Ebbinghaus, O. Krikorian, J. Lian, L. M. Wang and J. G. Catalano, *J. Nucl. Mater.*, 2002, **303**, 226–239.
43 X. Guo, S. V. Ushakov, S. Labs, H. Curtius, D. Bosbach and A. Navrotsky, *Proc. Natl. Acad. Sci. U. S. A.*, 2014, **111**, 17737–17742.
44 X. Guo, S. Szenknect, A. Mesbah, S. Labs, N. Clavier, C. Poinssot, S. V. Ushakov, H. Curtius, D. Bosbach, R. C. Ewing, P. C. Burns, N. Dacheux and A. Navrotsky, *Proc. Natl. Acad. Sci. U. S. A.*, 2015, **112**, 6551–6555.
45 X. Guo, D. Wu, H. Xu, P. C. Burns and A. Navrotsky, *J. Nucl. Mater.*, 2016, **478**, 158–163.
46 J. M. McHale and A. Navrotsky, *Chem. Mater.*, 1997, **9**, 1538–1546.
47 W. Herrendorf and H. Bärnighausen, *HABITUS: program for the optimization of the crystal shape for the numerical absorption correction in X-SHAPE (version 1.06, Fa. Stoe, Darmstadt)*, Karlsruhe, Germany, 1996.
48 G. M. Sheldrick, *SHELX-97: program pakage for solution and refinement of crystal structures from X-ray diffraction data*, Univ. Göttingen, Germany, 1997.
49 T. Hahn, *International Tables for Crystallography*, Kluwer Academic Publishers, Dordrecht, Boston, London, 1992.
50 P. C. Burns, *Can. Mineral.*, 2005, **43**, 1839–1894.
51 S. D. Kelly, K. M. Kemner, J. Carley, C. Criddle, P. M. Jardine, T. L. Marsh, D. Phillips, D. Watson and W. M. Wu, *Environ. Sci. Technol.*, 2008, **42**, 1558–1564.
52 N. Belai, M. Frisch, E. S. Ilton, B. Ravel and C. L. Cahill, *Inorg. Chem.*, 2008, **47**, 10135–10140.
53 B. Kosog, H. S. La Pierre, M. A. Denecke, F. W. Heinemann and K. Meyert, *Inorg. Chem.*, 2012, **51**, 7940–7944.
54 X. Guo, A. H. Tavakoli, S. Sutton, R. K. Kukkadapu, L. Qi, A. Lanzirotti, M. Newville, M. Asta and A. Navrotsky, *Chem. Mater.*, 2014, **26**, 1133–1143.
55 R. A. Robie and B. S. Hemingway, *Thermodynamic properties of minerals and related substances at 298.15 K and 1 bar pressure and at higher temperatures*, 1995.
56 T. I. Panova, E. N. Isupova and E. K. Keler, *Inorg. Mater.*, 1978, **14**, 616–617.
57 R. Guillaumont, T. Fanghänel, J. Fuger, I. Grenthe, V. Neck, D. A. Palmer and M. H. Rand, *Update on the Chemical Thermodynamics of Uranium, Neptunium, Plutonium, Americium and Technetium*, Elsevier, 2003, ch. 5, pp. 45–46.
58 M. W. J. Chase, *J. Phys. Chem. Ref. Data*, 1998, 1–1951, Monograph 9.